# Double Star Measurements at the Southern Sky with 50 cm Reflectors and Fast CCD Cameras in 2012

Rainer Anton

Altenholz/Kiel, Germany
e-mail: rainer.anton"at"ki.comcity.de

**Abstract**: A Cassegrain and a Ritchey-Chrétien reflector, both with 50 cm aperture, were used in Namibia for recordings of double stars with fast CCD cameras and a notebook computer. From superposition of "lucky images", measurements of 39 double and multiple systems were obtained and compared with literature data. Occasional deviations are discussed. Images of some remarkable systems are also presented.

## Introduction

As in earlier work, the technique of "lucky imaging" was applied to effectively reduce seeing effects during recording of double star images by using short exposure times. With only the best frames being registered and stacked, the resolution can approach the theoretical limit of the telescope, and the accuracy of position measurements can even be better than this by about one order of magnitude. In this paper, measurements on double and multiple systems made in fall 2012 are reported. Star brightness range is mostly above 8 mag, and only in a few cases, some dimmer companions are also imaged. While some systems are sufficiently well documented in the literature, and can be used for calibration of the image scale, in the majority of cases, data are scarce or exhibit large scatter. About 31 pairs are binaries with more or less well known orbits. In some cases, deviations from ephemeris data are found and possible causes are discussed.

## Instrumental

Most recordings were made with a 50 cm telescope of Ritchey-Chrétien type (*Alluna*, Germany), which has recently been installed at the *Internationale Amateur-Sternwarte* (IAS) in Namibia [1]. The focal length is 4.1 m. Some additional observations were done with a 50 cm Cassegrain with focal length 4.5 m, which I have already used in earlier years [2]. For most recordings, the magnification was about doubled with a Barlow lens. Imaging was done with two b/w-CCD cameras, one of type DMK31AF03 (*The Imaging Source*), and the other of type "Chameleon" (*Point Grey*). The main difference is the number and size of the pixels, 1024 x 768 of 4.65 µm square for the DMK31, and 1296 x 964 of 3.75 µm for the Chameleon. While the smaller pixel size of the latter helps in resolving close doubles, it produces somewhat more noise which, however, does virtually no harm in short exposures. Resolution values in terms of arcsec per pixel for the combinations of telescopes and cameras are listed in Table 1 below. These scaling factors were obtained with calibration stars (see Table 2 below), and agree with calculated values and/or earlier results within the error limits.

Position angles are measured as usual by recording trails in east-west direction, while the telescope drive was temporarily switched off.

Generally, I used a red or near infrared filter to reduce seeing effects and the atmospheric spectrum, and

*Table 1: Resolution values in arcsec/pixel for combinations of telescopes and cameras, with and without a nominal 2x Barlow lens. Ratios agree with earlier measurements within the error limits of about ± 0.5%. Likewise, the ratio for the two cameras corresponds to the ratio of the pixel sizes.*

| camera | DMK31 | | Chameleon |
|---|---|---|---|
| telescope | w/o B | w B | w/o B |
| 50 cm Cassegrain | 0.212 | not used | 0.171 |
| 50 cm RC | 0.234 | 0.121 | not used |

especially when using the Barlow lens, to reduce chromatic aberration. A few systems with color contrast were in addition recorded with green and blue filters in order to produce RGB composite images. Exposure times varied between 0.5 msec and 100 msec, depending on the star brightness. Under good seeing conditions, some systems were also recorded with exposures up to 2 sec, in order to image faint companions. In cases of large differences of brightness of the components, the main star became overexposed, and its position could eventually be determined by the diffraction spikes from the secondary mirror cell. More details of the technique and image processing are for example described in ref. [3].

## Results

All measurements are listed in Table 2, which is followed by individual notes. Numbering of the notes (last column at right) is with rounded R.A. values, which may make locating in the listings easier. Names, position and magnitude data are taken from the *WDS* [4]. Several systems were recorded with different configurations of telescope/camera. Measures of the position angle, P.A., and of the separation, rho, were then averaged. N is the total number of recordings. Shaded lines denote systems which were used for calibration of the image scale (see below). The residuals, delta P.A. and delta rho, refer to the trends of literature data, if sufficiently available, or for binaries, to the currently assumed ephemeris. Main sources are the *Fourth Catalog of Interferometric Measurements of Binary Stars ("speckle catalog")* [5], and the *Sixth Catalog of Orbits of Visual Binary Stars* [6]. Data available up to early 2014 are taken into account, as of writing this article. In several cases, larger deviations were found, which often agree with trends of literature data, however. These will be discussed in more detail below. In other cases, literature data are so scarce and/or exhibit so large scatter that no reasonable residuals can be given.

## Discussion

In Table 1, systems used for calibration of the image scale are marked with shaded lines, and comprise both measurements with and without Barlow. In Figures 1 and 2, for data obtained using the 50cm RC, individual residuals are plotted separately, partly in order to demonstrate that the calibration constants for both modes, as given above in the section *Instrumental*, are consistent. Data points on or close to the zero line are used for calibration by averaging. Some systems exhibit significant deviations which are discussed in the notes or below.

Generally, and according to earlier work, error margins for separation measurements are expected to be of the order of ±0.02 arcsec, and not to exceed ±0.05 arcsec,

*(Continued on page 237)*

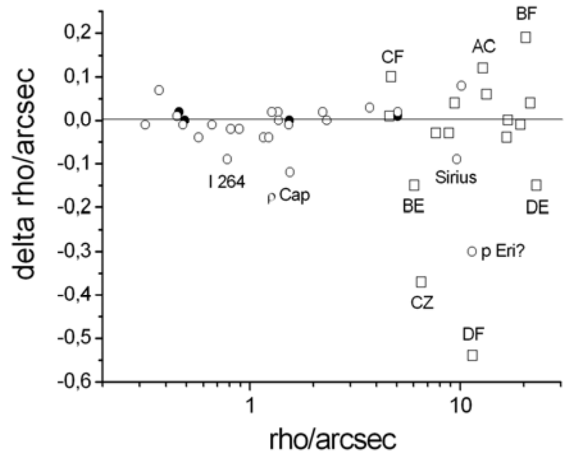


*Fig. 1: Plot of the residuals of rho versus rho (50cm RC with DMK31 camera). Semi-logarithmic scale. Open symbols refer to recordings with Barlow, full dots to no Barlow. Open squares are data for the trapezium in Orion (see text). Some systems with large deviations are marked with their names, or for pairs in the trapezium with their designations. See also notes.*

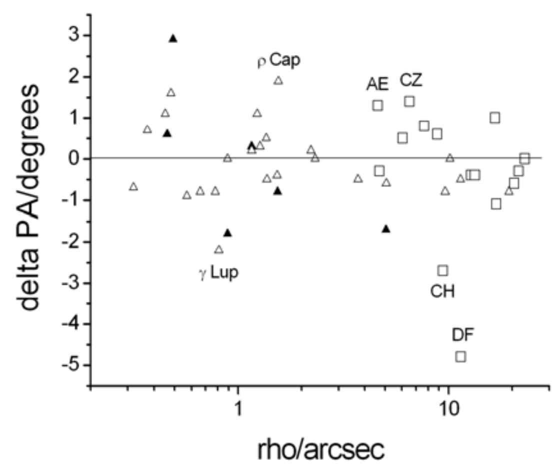


*Fig. 2: Plot of the residuals of the P.A. versus rho (50cm RC with DMK31 camera). Semi-logarithmic scale. Open symbols refer to recordings with Barlow, full triangles to no Barlow. Open squares are data for the trapezium in Orion (see text). Some systems with large deviations are marked with their names. Binaries gamma Lupi and rho Capricorni exhibit highly inclined orbits. See also notes.*

*Table 2: List of all measurements. Systems used for calibration of the image scale are marked by shaded lines. Position angles (P.A.) are in degrees, separations (rho) in arcseconds. N is the number of different recordings. Residuals delta P.A. and/or delta rho are given, when extrapolations of literature data appear reasonable. Notes with asterisks refer to figures shown below.*

| PAIR | RA + DEC | MAGS | P.A. meas. | rho meas. | DATE | N | delta P.A. | delta rho | NOTES |
|---|---|---|---|---|---|---|---|---|---|
| SLR 1 AB | 01 06.1 -46 43 | 4.10 4.19 | 98.1 | 0.48 | 2012.71 | 3 | +1.6 | -0.01 | 01 06* |
| HJ 3423 AB | 01 15.8 -68 53 | 5.00 7.74 | 316.3 | 4.74 | 2012.70 | 1 | -1.6 | -0.22 | 01 16 |
| I 27 CD | | 7.84 8.44 | 324.3 | 1.05 | 2012.70 | 1 | +2.5 | -0.05 | |
| I 264 AB | 01 31.6 -53 22 | 8.36 8.84 | 29.0 | 0.78 | 2012.72 | 1 | -0.8 | -0.09 | 01 32 |
| DUN 5 | 01 39.8 -56 12 | 5.78 5.90 | 187.3 | 11.39 | 2012.71 | 1 | -0.5 | -0.30 | 01 40 |
| JC 8 AB<br>HJ 3556 AC | 03 12.4 -44 25 | 6.42 7.36<br>6.42 8.76 | 156.7<br>188.6 | 0.57<br>3.75 | 2012.72 | 1<br>1 | -0.9<br>* | -0.04<br>* | 03 12* |
| BU 1004 | 04 02.1 -34 29 | 7.26 7.94 | 57.4 | 1.16 | 2012.720 | 2 | +0.2 | -0.04 | 04 02 |
| HJ 3683 | 04 40.3 -58 57 | 7.33 7.45 | 89.2 | 3.71 | 2012.721 | 1 | -0.5 | +0.03 | 04 40 |
| STT 98 | 05 07.9 +08 30 | 5.76 6.67 | 294.9 | 0.89 | 2012.721 | 1 | ~0 | -0.02 | 05 08* |
| STT 517 | 05 13.5 +01 58 | 6.79 6.99 | 240.8 | 0.66 | 2012.721 | 1 | -0.8 | -0.01 | 05 14 |
| STF 668 A,BC | 05 14.5 -08 12 | 0.3 6.8 | 204.9 | 9.53 | 2012.721 | 1 | * | * | 05 15 |
| STF 748 AB | 05 35.3 -05 23 | 6.55 7.49 | 31.6 | 8.87 | 2012.721 | 2 | +0.6 | -0.03 | 05 35* |
| STF 748 AC | | 6.55 5.06 | 131.6 | 12.82 | | 2 | -0.4 | +0.12 | |
| STF 748 AD | | 6.55 6.38 | 95.7 | 21.44 | | 2 | -0.3 | +0.04 | |
| STF 748 AE | | 6.55 11.1 | 352.3 | 4.61 | | 1 | +1.3 | +0.01 | |
| STF 748 BC | | 7.49 5.06 | 162.9 | 16.80 | | 2 | -1.1 | ~0 | |
| STF 748 BD | | 7.49 6.38 | 120.2 | 19.29 | | 2 | -0.8 | -0.01 | |
| STF 748 BE | | 7.49 11.1 | 240.5 | 6.05 | | 1 | +0.5 | -0.15 | |
| STF 748 BF | | 7.49 11.5 | 153.4 | 20.49 | | 1 | -0.6 | +0.19 | |
| STF 748 CD | | 5.06 6.38 | 61.6 | 13.36 | | 2 | -0.4 | +0.06 | |
| STF 748 CE | | 5.06 11.1 | 322.0 | 16.56 | | 1 | +1.0 | -0.04 | |
| STF 748 CF | | 5.06 11.5 | 119.7 | 4.70 | | 1 | -0.3 | +0.10 | |
| STF 748 CG | | 5.06 16.7 | 33.8 | 7.67 | | 1 | +0.8 | -0.03 | |
| STF 748 CH | | 5.06 15.8 | 269.3 | 9.44 | | 1 | -2.7 | +0.04 | |
| STF 748 CZ | | 5.06 12.7 | 338.4 | 6.53 | | 1 | +1.4 | -0.37 | |
| STF 748 DE | | 6.38 11.1 | 287.0 | 22.95 | | 1 | ~0 | -0.15 | |
| STF 748 DF | | 6.38 11.5 | 221.2 | 11.46 | | 1 | -4.8 | -0.54 | |
| DUN 23 | 06 04.8 -48 28 | 7.30 7.69 | 127.4 | 2.60 | 2012.70 | 1 | +2.6 | +0.12 | 06 05 |
| R 65 AB | 06 29.8 -50 14 | 5.97 6.15 | 257.8 | 0.53 | 2012.70 | 1 | ~0 | +0.01 | 06 30 |
| HDO 195 CD | | 7.98 8.73 | 159.2 | 0.38 | 2012.70 | 1 | -3.2 | +0.01 | 06 30 |
| DUN 30 AB,CD | | 5.97 7.98 | 311.7 | 11.77 | 2012.70 | 1 | <0.3 | ~0 | 06 30 |
| AGC 1 AB | 06 45.1 -16 43 | -1.46 8.5 | 83.1 | 9.63 | 2012.72 | 1 | -0.8 | -0.09 | 06 45 |
| DUN 252 AB | 12 26.6 -63 06 | 1.25 1.55 | 111.9 | 3.85 | 2012.70 | 2 | -1.3 | -0.01 | 12 27* |
| DUN 252 AC | | 1.25 4.80 | 202.2 | 89.6 | 2012.70 | 3 | ~0 | * | 12 27* |
| ANT 1 AG | | 1.25 10. | 145.6 | 56.4 | „ | 1 | -0.4 | -0.3 | 12 27* |
| ANT 1 AH | | 1.25 13. | 166.7 | 47.3 | „ | 1 | -0.3 | -0.1 | 12 27* |
| ANT 1 AI | | 1.25 12. | 227.1 | 63.3 | „ | 1 | +0.1 | -0.6 | 12 27* |
| RHD 1 AB | 14 39.6 -60 50 | 0.14 1.24 | 262.7 | 5.05 | 2012.71 | 5 | -0.6 | +0.02 | 14 40 |

*Table 2 concludes on next page.*

*Table 2 (conclusion): List of all measurements. Systems used for calibration of the image scale are marked by shaded lines. Position angles (P.A.) are in degrees, separations (rho) in arcseconds. N is the number of different recordings. Residuals delta P.A. and/or delta rho are given, when extrapolations of literature data appear reasonable. Notes with asterisks refer to figures shown below.*

| PAIR | RA + DEC | MAGS | P.A. meas. | rho meas. | DATE | N | delta P.A. | delta rho | NOTES |
|---|---|---|---|---|---|---|---|---|---|
| HJ 4786 | 15 35.1 -41 10 | 2.95 4.45 | 274.6 | 0.81 | 2012.72 | 1 | -2.2 | -0.02 | 15 35 |
| COO 193 | 16 07.7 -38 02 | 8.97 8.99 | 224.0 | 1.87 | 2012.72 | 1 | * | * | 16 08 |
| BU 120 AB | | 4.35 5.31 | 3.1 | 1.36 | 2012.72 | 1 | +0.5 | +0.02 | |
| H 5 6 AC | 16 12.0 -19 28 | 4.35 6.60 | 336.2 | 41.37 | 2012.72 | 1 | * | * | 16 12 |
| MTL 2 CD | 16 12.0 -19 28 | 6.60 7.23 | 55.5 | 2.32 | 2012.72 | 1 | ~0 | ~0 | 16 12 |
| BSO 13 AB | 17 19.1 -46 38 | 5.61 8.88 | 256.9 | 10.15 | 2012.73 | 1 | ~0 | +0.08 | 17 19 |
| I 252 | 19 01.5 -34 30 | 8.70 8.80 | 50.2 | 0.85 | 2012.70 | 1 | * | * | 19 01 |
| HDO 150 AB | 19 02.6 -29 53 | 3.27 3.48 | 271.2 | 0.45 | 2012.71 | 4 | +1.1 | +0.01 | 19 02* |
| HU 261 | 19 04.3 -21 32 | 7.87 8.06 | 186.6 | 1.27 | 2012.71 | 2 | +0.3 | +0.02 | 19 04 |
| HJ 5084 | 19 06.4 -37 04 | 4.53 6.42 | 359.5 | 1.37 | 2012.72 | 1 | -0.5 | ~0 | 19 06 |
| GLE 3 | 19 17.2 -66 40 | 6.12 6.42 | 349.6 | 0.51 | 2012.70 | 1 | +3.0 | -0.01 | 19 17 |
| I 253 | | 8.77 7.25 | 143.8 | 0.37 | | 1 | +0.7 | +0.07 | |
| BU 142 | | 8.12 8.69 | 283.6 | 1.06 | | 1 | ~0 | +0.05 | |
| I 120 AB | | 8.31 8.02 | 187.5 | 0.39 | | 1 | +4.8 | -0.01 | |
| HU 5141 AB-C | | 7.36 10.4 | 340.4 | 11.84 | | 1 | * | * | |
| HDO 294 | | 8.08 9.11 | 30.8 | 1.19 | | 1 | -3.7 | -0.12 | |
| R 321 | | 6.58 8.09 | 127.0 | 1.54 | | 1 | +1.7 | -0.01 | |
| SHJ 323 AB | | 4.97 6.88 | 191.1 | 1.55 | | 1 | +1.9 | -0.12 | |
| HU 200 AB | 19 19.0 -33 17 | 5.38 7.31 | 120.5 | 0.32 | 2012.72 | 2 | -0.7 | -0.01 | 19 19* |
| HU 5319 | | 7.65 7.66 | 315.1 | 2.05 | | 1 | +0.1 | -0.05 | |
| SHJ 345 AB | | 6.29 6.39 | 51.6 | 1.23 | | 1 | +1.1 | -0.04 | |
| STF 2909 | | 4.34 4.49 | 167.4 | 2.22 | | 2 | +0.2 | +0.02 | |
| I 304 | | 8.50 8.72 | 0.9 | 4.08 | | 1 | * | * | |
| I 22 AB | | 7.29 8.91 | 175.0 | 0.56 | | 1 | ~0 | +0.04 | |
| JC 20 AB | | 4.45 6.60 | 114.9 | 1.53 | | 2 | -0.4 | -0.01 | |
| SLR 14 | | 8.28 8.59 | 65.7 | 0.94 | | 2 | -1.8 | -0.02 | |

Notes:

Terms “cpm” (common proper motion) and “relfix” (relatively fixed) refer to Burnham [7].

01 06: beta Phoenicis, binary, P = 168 y. See fig. 3.

01 16: kappa Tucanae, binary, P = 857 y, few data, own measure significantly deviates from currently assumed orbit, but seems to be consistent with earlier measurements from 2008 and 2009. Pair CD is close to kappa Tucanae, binary, P = 86 y. All cpm.

01 32: in Eridanus, AB binary, P = 250 y, rho AB deviates from ephemeris, but follows trend of literature data, too few data for AC.

01 40: p Eridani, binary, P = 484 y, although an easy pair, only few data in the literature.

03 12: in Eridanus, AB binary, P = 45 y, well documented with speckle data. See fig. 3.

04 02: in Eridanus, binary, P = 282 y, orbit calculation has recently been refined.

04 40: in Dorado, binary, P = 240 y, orbit highly inclined.

05 08: in Orion, binary, P = 199 y, many speckle data. See fig. 3.

05 14: in Orion, binary, P = 312 y, many speckle data.

05 15: Rigel, beta Orionis, relfix, large difference in brightness, few data.

05 35: theta$^1$ Orionis, “trapezium”, residuals given vs. last entries in the WDS (as of 2014-02), for pairs combining A, B, C and D from 2013, for AE and CF from 2009, for CE from 2008, for BE and BF from 2006, for DE from 2002, and for DF from 1987, see text.

06 05: in Puppis, binary, P = 464 y, measured position deviates from orbit, but follows the trend of speckle data.

06 30: in Puppis, also known as DUN 30 AB, CD: another “double-double” with two binaries: AB: P = 52.9 y, CD: P = 101 y, all cpm. The separation of the two pairs is decreasing. WDS data for DUN 30 seems to refer to AC.

06 45: Sirius, alpha Canis Majoris, famous binary, P = 50.9 y. Large difference in brightness of the components makes measurement difficult.

12 27: alpha Crucis, AB binary, but no orbit listed. While rho(AB) has been monotonously decreasing for more than 150 years, the last entry in the WDS of 3.6” from 2012 appears to be much lower than expected. No residuals for C given, because of too few data. Residuals of G, H, and I refer to own measurements of 2007.

14 40: alpha Centauri, AB binary, P = 79.9 y, well documented.

15 35: gamma Lupi, binary, P = 190 y, highly inclined orbit.

16 08: in Lupus, few data.

16 12: nu Scorpii, “double-double”, but no orbits known. Some scatter of data for AC.

17 19: also known as L 7194, in Ara, binary, P = 693.3 y.

19 01: in Sagittarius, few data, PA inc, rho slow dec ?, extrapolation ambiguous.

19 02: zeta Sagittarii, fast binary, P = 21.1 y. See fig. 3.

19 04: also known as H N 126, in Sagittarius, binary, P = 356 y.

19 06: gamma Coronae Australis, binary, P = 122 y, PA rapid inc, rho slow inc.

19 17: in Pavo, binary, P = 157 y.

19 19: in Sagittarius, binary, P = 60 y, highly inclined orbit, showcase, but only few data. See fig. 3.

19 28: in Sagittarius, binary, P = 162 y. Rho significantly deviates from actual ephemeris, but seems to follow the trend of literature data. See fig. 6.

19 49: in Pavo, AB binary, P = 61.1 y; AB-C: PA dec, all cpm, C physical. Few data, large scatter.

20 01: in Sagittarius, binary, P = 475 y, “premature orbit”, own measures significantly deviate from currently assumed orbit, but follow the trend of recent speckle data.

20 27: in Sagittarius, binary, P = 178 y.

20 29: rho Capricorni, binary, P = 278 y, orbit highly inclined, large residuals vs. ephemeris, own measure better follows the trend of recent speckle data.

20 39: tau$^2$ Capricorni, binary, P = 200 y, large scatter of literature data. See fig. 3.

22 12: in Grus, few data.

22 27: 53 Aquarii, binary, P = 3500 y?, despite the long period, PA is rapidly increasing with about 4 degrees/year, as the companion is near periastron, while rho is only slowly decreasing.

22 29: zeta Aquarii, binary (ternary), P = 760 y, position of B has been deviating from the ephemeris in recent years, due to the pull of a companion not seen in the visible, but is now again near the calculated orbit.

22 47: in Grus, few data with large scatter.

22 55: tau$^2$ Gruis, probably binary, no orbit, large variations of rho data, brightness ratio differs.

23 07: theta Gruis, cpm, PA and rho inc.

23 51: in Phoenix, binary, P = 117 y.

**Double Star Measurements at the Southern Sky with 50 cm Reflectors and Fast CCD Cameras ...**

*(Continued from page 233)*

at least in the range of small separations. As can be seen in Figure 1, several pairs are clearly off, and many of these are binaries. As the residuals are calculated with respect to the current ephemeris, deviations may indicate that this is not up to date. In fact, in many cases, residuals against the trend of recent measurements are found much smaller. An example is shown in Figure 6 below.

A special case seems to be the trapezium cluster in the constellation Orion. While data for the brighter pairs combining A, B, C, and D more or less agree with recent entries in the WDS (the most recent ones are from 2013), the positions of E and F significantly deviate from older data. However, because of the unknown error margins, no definite conclusions as to individual movements can be drawn so far. See also Figure 4.

The error margins of measurements of the position angle are expected to be of the order of about +/- 0.2 degrees for large separations, but to increase towards small separations, and can reach several degrees for very close pairs. The reason is the fixed resolution in the images. In fact, this is apparent in the plots in fig. 2. However, a number of pairs seem to stand out more than this, in particular binaries with highly inclined orbits, and again, several members of the trapezium cluster.

Possible origins of deviations of PA and rho are already mentioned in the notes list. In particular, the following binaries deserve further attention in the (near and far) future (in order of increasing R.A., listed here with the note numbers):

- 01 16: κ Tucanae,
- 01 32: I 264 AB in Eridanus,
- 01 40: DUN 5 (p) Eridani,
- 19 19: I 253 in Sagittarius,
- 19 28: SCJ 22 (BU 142) in Sagittarius,
- 20 01: HDO 294 in Sagittarius,
- 20 29: ρ Capricorni,
- 20 39: $\tau^2$ Capricorni
- 22 55: $\tau^2$ Gruis.

Some images of double and multiple systems are presented in the following figures. Figure 3 is a selection of close binaries with sub-arcsec separations.

*(Continued on page 239)*

*Figure 3. A selection of close binaries. 50 cm RC telescope. Image of JC 8 is overexposed and inverted in order to better show the dim companion C. See also notes 20 39, 19 19, 19 02, 01 06, 03 12, and 05 08, respectively. North is down, and east is right, as in all images.*

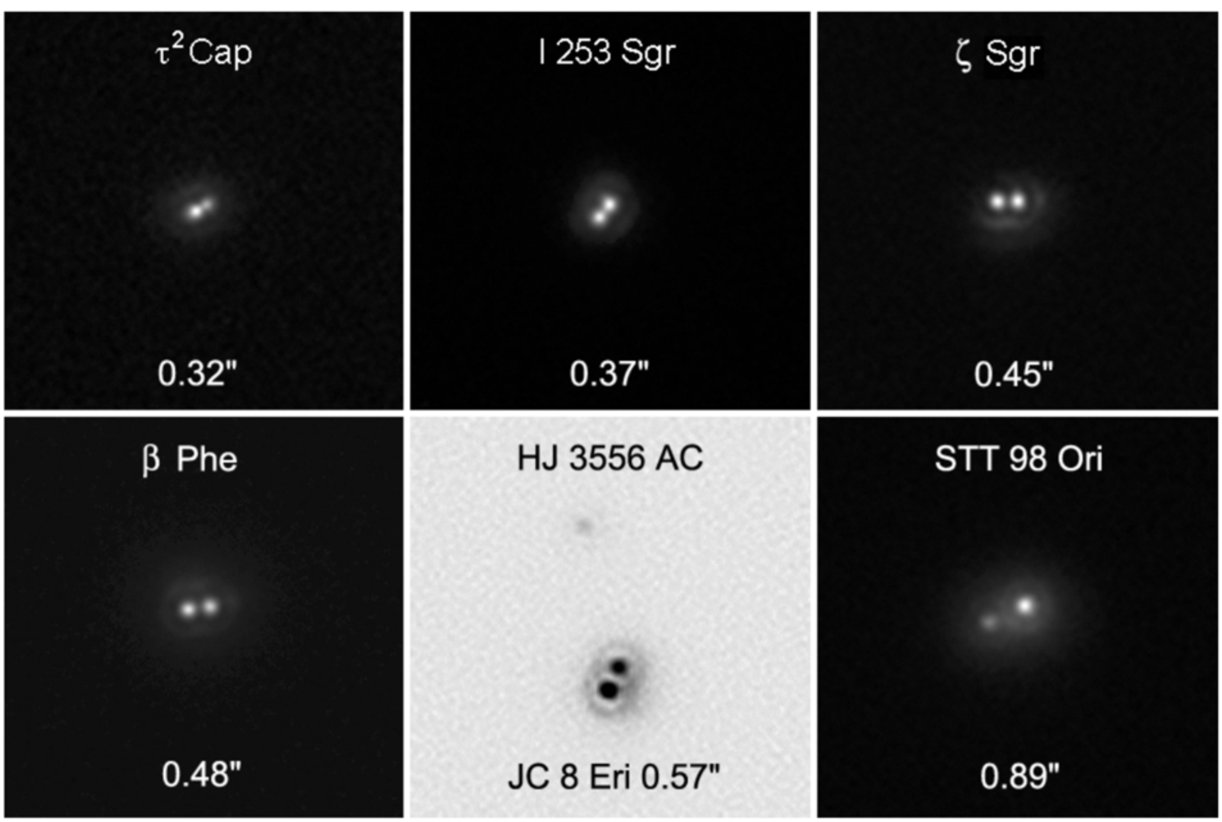

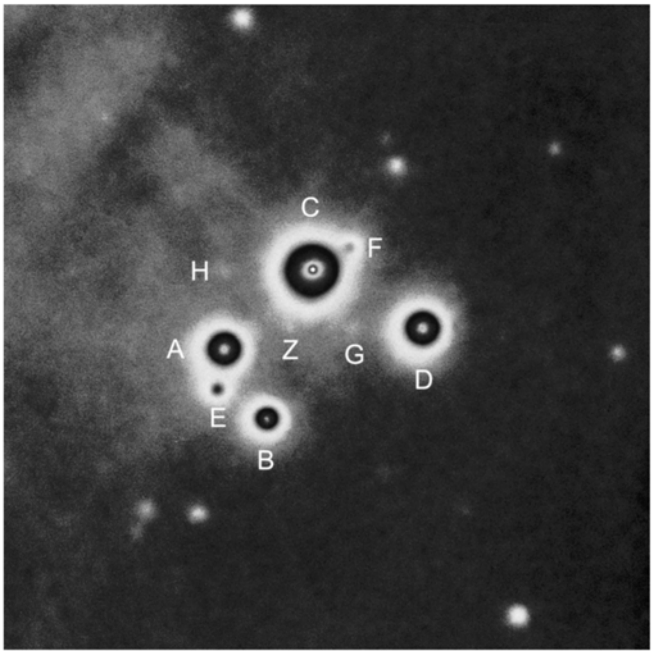


*Figure 4. The trapezium cluster in Orion. 50cm RC. Superposition of three images with different exposure times (~300 frames each with 20 msec, 100 msec, and 1 sec). The contrast was strongly enhanced, and partly reversed, so as to reveal both the relative positions of the brighter stars as well as of the dimmer ones. Components as listed in the WDS are indicated. Brightness of G is given as 16.7 mag. The one second image also shows parts of the nebula and several field stars. See text.*

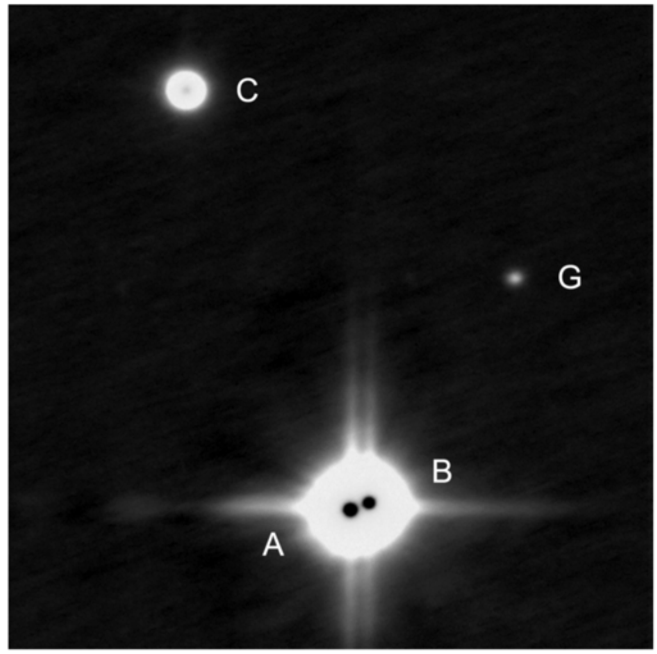


*Figure 5. ACRUX: Superposition of a 2sec exposure and a shorter exposure (as negative). Brightness of component G is estimated to about 10 mag. Even dimmer companions H and I are only seen with strongly enhanced contrast. See also note 12 27.*

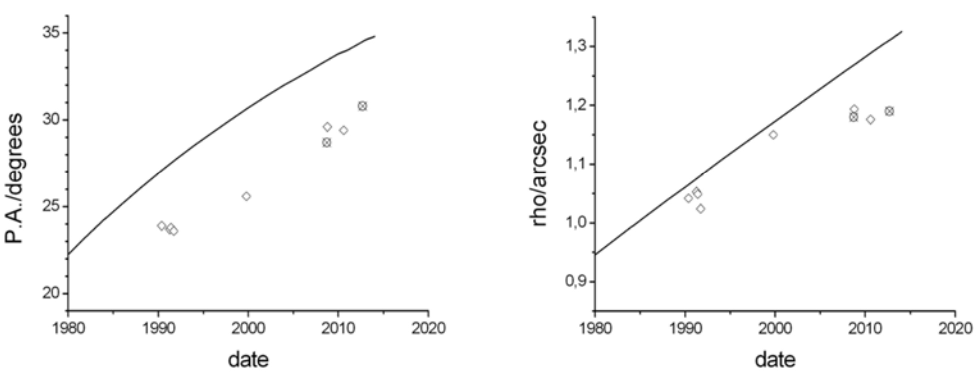


*Figure 6. Plots of position angle (left) and separation (right) of the pair HDO 294 vs. date. Rhombs are speckle data, crossed circles are own measurements. Curves indicate the currently assumed ephemeris. See also note 20 01.*

*(Continued from page 237)*

## Conclusion

For many of the doubles investigated here, there are only few data found in the literature, and often with large scatter, although most systems are fairly bright, and easily accessible. The accuracy of my own measurements is checked by comparing with mainly speckle data of systems, which have frequently been observed. Generally, the scatter is of comparable magnitude. As in earlier work, this measuring campaign again revealed several double star systems, which should be measured more often.

## References

[1] IAS, http://www.ias-observatory.org

[2] Anton, R., 2010, *Journal of Double Star Observations,* **vol. 6** (2), 133-140.

[3] Anton, R., 2012, Lucky imaging. In *Observing and Measuring Visual Double Stars, 2nd Edition*, Robert Argyle, ed., Springer, New York.

[4] Mason, B.D. et al., *The Washington Double Star Catalog (WDS)*, U.S. Naval Observatory, online access Feb. 2014.

[5] Hartkopf, W.I. et al., *Fourth Catalog of Interferometric Measurements of Binary Stars,* U.S. Naval Observatory, online access Feb. 2014.

[6] Hartkopf, W.I. et al., *Sixth Catalog of Orbits of Visual Binary Stars,* U.S. Naval Observatory, online access Feb. 2014.

[7] *Burnham´s Celestial Handbook,* R. Burnham, Jr., Dover Publications, New York 1978.